ENERGY DEPOSITION WITHIN SUPERCONDUCTING COILS OF A 4-MW TARGET STATION

N. Souchlas,* R.C. Fernow, H.G Kirk, BNL, Upton, NY 11973, USA,

R.J. Weggel, Particle Beam Lasers, Inc., Northridge, CA 91324, USA,

K.T. McDonald, Princeton University, Princeton, NJ 08544, USA,

X. Ding, UCLA, Los Angeles, CA 90095, USA,

J.J. Back, Warwick University, Coventry CV4 7AL, UK

Abstract

We present results from a study in which the magnet configuration and internal shielding against energy deposition by secondary particles is optimized for a 4-MW target station at a Muon Collider or Neutrino Factory.

INTRODUCTION

The intense 4-MW proton beam that drives a muon collider or neutrino factory [1] will create a shower of particles that irradiate different components of the target station [2, 3]. A 10-year operational lifetime is desired for the superconducting coils, which translates into a requirement that the peak power density deposition in them by secondary particles be only 0.15 mW/g [4]. The total power deposition in materials at 4K is also an important consideration. The configuration of the coils and internal shielding has been optimized with the aid of peak power density and total power calculated using the MARS15 code [5] with the MCNP code cross sections libraries [6]. The latter is important in providing a more detailed treatment of low-energy neutrons. Results will be compared with simulations using the FLUKA code [7].

STUDY II TARGET STATION GEOMETRY

The configuration of the target station of Neutrino Factory Study II [8] is shown in Fig. 1. A 4-MW, 8-GeV pulsed beam (50 Hz) of protons with Gaussian profile of $\sigma_x = \sigma_y = 0.12$ cm interacts with a free Hg jet with radius of 0.4 cm and speed of 20 m/s. Both the proton beam and the mercury jet are tilted with respect to the magnet axis to maximize collection of low-energy pions. A total of thirteen superconducting (SC) coils and three resistive coils create the desired magnetic field. The three resistive coils around the target area will provide 6-T magnetic field so the peak field in the NbSn superconductor is only 14 T. The superconducting coils are shielded by tungsten-carbide (WC) beads cooled by water. Coil SC#1 around the target area has an inner radius of 63.3 cm and is shielded from
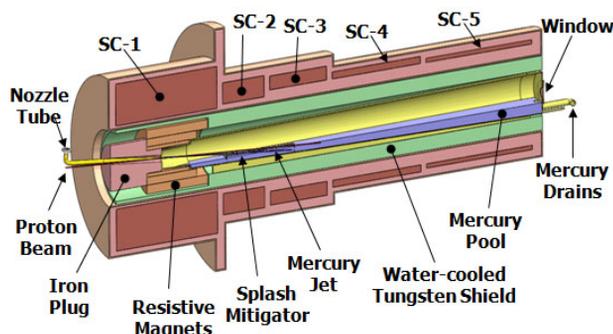
_____
* nsouchlas@bnl.gov

Figure 1: Neutrino Factory Study II [8] concept of a 4-MW target station based on a free-mercury jet inside at 20-T solenoid. The superconducting coils are protected from secondary particles by an internal shield of water-cooled WC beads.

the target by the resistive coils and a small annulus of WC beads inside them.

Initial studies with the MARS15 code [9] with the default neutron-energy cutoff of 0.1 MeV, and for the initial shielding packing ratio, indicated that about 25 kW power would be deposited in coil SC#1, and the total power deposited in the 13 SC coils would be 37 kW. Energy-deposition results from a FLUKA simulation were about a factor of 2 higher. On using MARS15 with the MCNP package and a neutron energy cutoff of 10^{-11} MeV, the power deposited in the coil SC#1 was calculated to be 43 kW while the total power deposited in all 13 SC coils would be 58 kW and there is better agreement with FLUKA. The peak energy deposition in the coil SC#1 would be about 6 mW/g, corresponding to a lifetime of one month against radiation damage. If the three resistive coils, of 30 cm radial thickness, were replaced with shielding material the power deposition in coil SC#1 would be reduced to 13 kW.

Figure 2 shows the power deposited in coil SC#1, with and without shielding when the cutoff on the minimum neutron energy in the simulation is varied. While most of the deposited power originates with neutrons of $E > 1$ MeV, some 10% is associated with thermal neutrons.
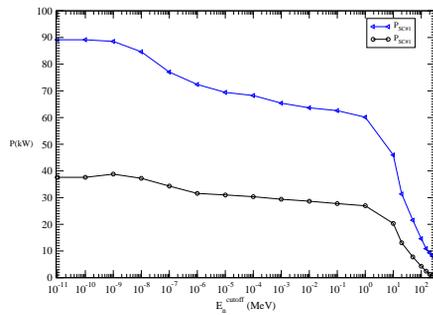
Accelerator Technology

Figure 2: Power deposited in SC#1, with and without shielding material, as a function of the neutron energy cut-off from 10^{-11} to 300 MeV in a MARS/MCNP simulation.
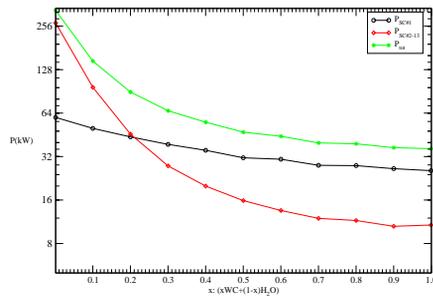

Figure 3: Power deposited in SC#1, SC#2-13, and in all SC coils, as a function of the volume fractions of WC and water in the shielding material (MARS/MCNP).

An implication is that the task of additional shielding will be primarily to suppress MeV neutrons, rather than thermal neutrons. Additional evidence for this interpretation is given in Fig. 3, which shows the simulated power deposition in coils SC#1, SC#2-13 and in all coils, supposing that the shield could be varied between pure WC and pure water. It is better to have more, dense WC shielding, which is effective against higher-energy neutrons, than to increase the fraction of water. A shield composed of spherical beads of a fixed radius will have about 40% void fraction, which becomes filled with water. The simulation indicates that while it would be slightly better to have a smaller fraction of water than this, the combination of 60% WC and 40% water is a good shield.

INCREASED SHIELDING

More shielding of the SC coils compared to that in the Study II configuration is needed to ensure a 10-year lifetime against radiation damage. Five new configurations were studied with inner radii of the cryostat of SC magnets around the target varied between 80 and 120 cm. The additional radial space inside the SC coils was filled with WC and water (60/40) shielding, and shielding was added inside the SC coils between 6 and 16 m from the target (which previously had none).

Figure 4 illustrates the first and last of these configurations, IDS80f (top) and IDS120f (bottom). The number of
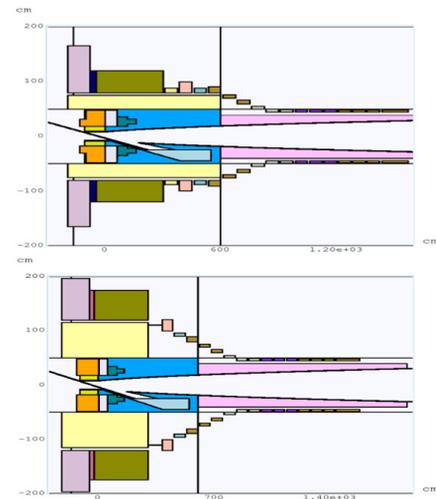

Figure 4: YZ plane cross section for IDS80f (top) and IDS120f (bottom) geometries.

resistive coils was increased from 3 to 5, and the number of SC coils was increased from 13 to 19, and their geometries and current densities chosen to maintain good field uniformity on the target and acceptable hoop stresses in the coils. The stored magnetic energy in these new configurations varies from 2 to 4 GJ.

MARS/MCNP simulations (with statistical uncertainty of 10-15%) of the peak power density deposited by secondary particles in coil SC#3, and the total power deposited in all SC coils, are shown in Fig. 5.
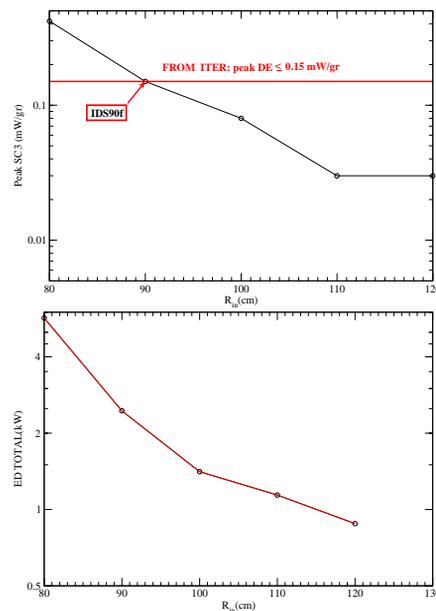

Figure 5: Peak power density in SC#3 (top) and total power deposited in all SC coils (bottom) as a function of the inner radius of coil #3 (IDS80-120f geometries).

Table 1: Power (in kW) deposited in different regions of the IDS120f target station from MARS15/MCNP and FLUKA codes. The Be window is 6.0 m downstream of the target.

TOTALS	MARS15	FLUKA
SC#1-19	0.97	0.56
SH#1-4	2020.06	2148.9
RS#1-5	329.55	405.1
BP#1-3	458.39	482.8
Hg TARG.	376.5	319
Hg POOL	10.16	4.4
Be WIND.	0.53	2.1
TOTAL	3196.16	3362.86

According to simulation of peak power density (Fig. 5 top), the IDS90f geometry satisfies the ITER criterion [4], although it is anticipated the more detailed design of the resistive magnets will require additional radial space of ≈ 10 cm for the magnet leads and cooling manifolds. The total thermal load at 4K remains about 1 kW even for the IDS120f configuration. To lower the thermal load, and permit all SC coils to be lifetime components (> 30 years), we have adopted the IDS120f configuration as the new baseline.

NEW BASELINE

For the new baseline [2] geometry (IDS120f) Fig. 4 (bottom) MARS15/MCNP simulation indicates that most of the 1-kW power deposited in the 19 SC coils is in SC#3 (0.26 kW) and SC#5 (0.19 kW), and the peak value of power density in SC#3 is 0.03 mW/g. The total power deposited in the SC coils (SC), shielding material (SH), resistive coils (RS), and beam pipe (BP), as well as in other parts of the target station are presented and compared with FLUKA results in Table 1. Figure 6 illustrates power de-
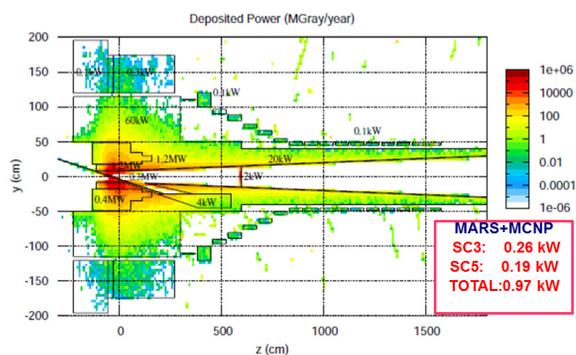

Figure 6: Power deposition in MGray/year and in kW in various regions of the IDS120f configuration as calculated in a FLUKA simulation. The insert compares results from MARS/MCNP for the two coils with the highest power deposition.

position in various regions of the IDS120f configuration as calculated in a FLUKA simulation. The two codes generally agree to within 10%, although the discrepancies are larger in the regions with smaller power deposition. The WC + H_2O shield (total mass ≈ 100 ton) must dissipate about 2 MW, and its 1-cm-thick stainless steel shell must dissipate over 400 kW. Some 200 kW must be dissipated in the small annulus of WC shielding inside the resistive magnets. The mercury jet absorbs about 10% of the beam power. Note that $\approx 20\%$ of the beam power is transmitted into the downstream beam elements.

CONCLUSIONS

Use of MCNP cross section libraries coupled to the MARS15 code provides a better treatment of low energy neutrons. This has resulted in better agreement with FLUKA simulations. We found that excessive power would be deposited in the superconducting coils in the Study II geometry [1] , making their operation problematic. We studied a series of geometries (IDS80-120f) with larger inner radius of coils SC#1-3 to allow additional shielding and better access for services in the target station. The IDS120f geometry was found to satisfy the ITER criterion [4] for the peak density of deposited power and provides and operational lifetime against radiation damage in excess of 10 years.

ACKNOWLEDGMENTS

REFERENCES

[1] M.M. Alsharo'a *et al.*, "Status of Neutrino Factory and Muon Collider Research and Development and Future Plans", Phys. Rev. ST Accel. Beams **6**, 081001 (2003).

[2] H.G. Kirk, K.T. McDonald, "Target System Baseline" (Feb. 4, 2011), puhep.princeton.edu/~mcdonald/mumu/target/

[3] H.G. Kirk *et al.*, "A Solenoid Capture system for a Muon Collider", these proceedings, TUP265.

[4] J.H. Schultz, "Radiation Resistance of Fusion Magnet Materials", IEEE Symp. Fusion Energy, 423 (2003).

[5] The MARS Code System: http://www-ap.fnal.gov/MARS/

[6] The MCNP Code System: http://mcnp-green.lanl.gov/

[7] The official FLUKA site:http://www.fluka.org/fluka.php

[8] S. Ozaki *et al.*, "Feasibility Study II of a Muon-Based Neutrino Source" (June 14, 2001), http://www.cap.bnl.gov/mumu/studyii/FS2-report.html

[9] X. Ding, "Energy Deposition of 4-MW Beam Power in a Mercury Jet Target" (Feb. 9, 2010), puhep1.princeton.edu/~mcdonald/mumu/target/Ding/ding_020910.pdf